Chiral Metamaterials with *PT* Symmetry and Beyond

Sotiris Droulias,[1,2,*] Ioannis Katsantonis,[1,2] Maria Kafesaki,[1,2,†] Costas M. Soukoulis,[1,3] and Eleftherios N. Economou[1,4]
[1]*Institute of Electronic Structure and Laser, Foundation for Research and Technology Hellas, 71110 Heraklion, Crete, Greece*
[2]*Department of Materials Science and Technology, University of Crete, 71003 Heraklion, Greece*
[3]*Ames Laboratory and Department of Physics and Astronomy, Iowa State University, Ames, Iowa 50011, USA*
[4]*Department of Physics, University of Crete, 71003 Heraklion, Greece*

(Received 12 November 2018; published 28 May 2019)

Optical systems with gain and loss that respect parity-time (*PT*) symmetry can have real eigenvalues despite their non-Hermitian character. Chiral systems impose circularly polarized waves which do not preserve their handedness under the combined space- and time-reversal operations and, as a result, seem to be incompatible with systems possessing *PT* symmetry. Nevertheless, in this work we show that in certain configurations, *PT* symmetric permittivity, permeability, and chirality is possible; in addition, real eigenvalues are maintained even if the chirality goes well beyond *PT* symmetry. By obtaining all three constitutive parameters in realistic chiral metamaterials through simulations and retrieval, we show that the chirality can be tailored independently of permittivity and permeability; thus, in such systems, a wide control of new optical properties including advanced polarization control is achieved.

DOI: 10.1103/PhysRevLett.122.213201

The field of parity-time-reversal (*PT*) symmetry, initially introduced in the context of quantum mechanics [1–4], has attracted increasing interest because, according to this concept, it is possible even for non-Hermitian Hamiltonians to exhibit real eigenvalues. This occurs if the potential V satisfies $V(\mathbf{r}-\mathbf{r_0}) = V^*(-\mathbf{r}+\mathbf{r_0})$, where $\mathbf{r}$ is the position operator and $\mathbf{r_0}$ is the point with respect to which the parity transformation is defined (the asterisk denotes the complex conjugate). The eigenvalues remain real below some critical value of the potential, the so-called exceptional point, above which they become complex. Because paraxial beam propagation is described by a Schrödinger-like equation, the *PT* concept quickly found fertile ground in optics, where the required loss is naturally occurring and gain can be easily introduced; there, the role of the potential is played by the refractive index n and therefore $n(\mathbf{r}-\mathbf{r_0}) = n^*(-\mathbf{r}+\mathbf{r_0})$ [5–11]. The extension of *PT* symmetry to systems in which the space reversal is along the propagation direction and the eigenvalues refer to those of the scattering matrix [12–21] led to novel phenomena, such as coherent perfect absorption [13,14], the *PT*-laser absorber [15,16], and anisotropic transmission resonances [18]. Most recently, some works combined *PT* symmetry with metamaterials [22–28], which could extend these ideas to new limits; however, an important class of metamaterials, namely chiral metamaterials (CMMs) [29–37], remains highly unexplored in the context of *PT* symmetry.

In this work, prompted by both the enhanced polarization control capabilities of chiral metamaterials and the novel effects associated with *PT*-symmetric systems, we attempt to combine both features in the same system; our goal is to transfer the *PT*-related phenomena to waves of arbitrary polarization, from linear to circular, and to achieve advanced polarization control capabilities, as compared to those offered by passive chiral metamaterials. As a first step, we derive the necessary conditions for a chiral system to be *PT* symmetric; then for the system shown in Fig. 1, we obtain the full scattering matrix for arbitrary values of the constitutive coefficients (ε, μ, κ); next we examine how the obtained general results are modified if *PT* invariance is imposed. To our surprise, we find that both the eigenvalues and the *PT*-related functionalities are still preserved, independently of whether the *PT* requirement is violated in κ. This is unexpected, since it is only natural for the

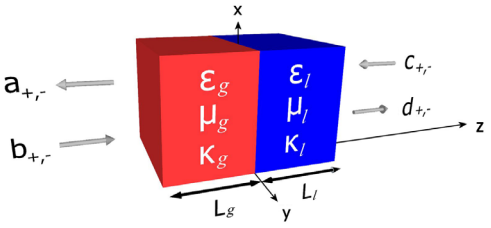

FIG. 1. A system of two homogeneous chiral slabs for the realization of a chiral *PT*-symmetric structure. The complex material parameters ε_i, μ_i, and κ_i are the relative permittivity, the relative permeability, and the chirality parameter, respectively, and the subscript $i = \{g, l\}$ denotes whether they are located in the "gain" or the "loss" region. For *PT* symmetry the shown parameters should satisfy $\varepsilon_g = \varepsilon_l^*$, $\mu_g = \mu_l^*$, $\kappa_g = -\kappa_l^*$, and $L_g = L_l$. The amplitudes of the incident (b, c) and scattered (a, d) waves are shown, where the subscript $+$ $(-)$ accounts for right- (left-) circularly polarized [RCP (LCP)] waves.

results to depend on the additional constitutive parameter (κ) as well, and not to be tuned solely via ε and μ. However, this result turns out to be of utmost importance for chiral systems, because it allows retaining an unbroken PT phase with all its benefits and controlling the chirality simultaneously and independently from the PT-related functionalities, thus enabling new optical capabilities, such as anisotropic transmission resonances with polarization conversion and unidirectional polarization conversion with no reflection, as we demonstrate explicitly. Finally, by simulations and retrieval we obtain various sets of values of the constitutive coefficients in realistic chiral metamaterials possessing either PT symmetry or extensions beyond this symmetry; these sets of values are such as to demonstrate that all our theoretical findings can take place in actual systems.

To find the conditions for PT symmetry in systems with chiral response, we cast Maxwell's equations $\nabla \times \mathbf{E} = i\omega\mathbf{B}$, $\nabla \times \mathbf{H} = -i\omega\mathbf{D}$ combined with the constitutive relations $\mathbf{D} = \varepsilon\varepsilon_0\mathbf{E} + i(\kappa/c)\mathbf{H}$ and $\mathbf{B} = \mu\mu_0\mathbf{H} - i(\kappa/c)\mathbf{E}$ [38] into an eigenproblem with a Schrödinger-like Hamiltonian (ε, μ are the relative permittivity and permeability, respectively, κ is the chirality parameter expressing the magnetoelectric coupling, and c is the vacuum speed of light, see Supplemental Material [39]). To achieve PT symmetry, first we require that the Hamiltonian $\bar{\bar{H}}$ commutes with the PT operator and then we investigate how the eigenvectors of $\bar{\bar{H}}$ are transformed under the action of space and time reversal. For a PT-symmetric Hamiltonian with nondegenerate spectrum to have real eigenvalues, the eigenvectors $\mathbf{F}$ should also be PT symmetric [21]; i.e., $PT\mathbf{F} = \mathbf{F}$. In our case, the eigenvectors of $\bar{\bar{H}}$ appear as pairs of right-circularly polarized [RCP or (+)] and left-circularly polarized [LCP or (−)] waves denoted as $\mathbf{F}_+$, $\mathbf{F}_-$, and, while time reversal ($t \to -t$) does not affect their handedness, the action of space reversal ($r \to -r$) transforms it between left and right, thus implying an apparent incompatibility of chiral systems with PT symmetry. However, because $\mathbf{F}_\pm$ share a common (degenerate) eigenvalue ω (i.e., $\bar{\bar{H}}\mathbf{F}_\pm = \omega\mathbf{F}_\pm$), this can be real if certain symmetries are preserved. For example, as is shown in the Supplemental Material [39], Sec. I, if the action of the PT operator maps RCP waves onto LCP waves and vice versa ($PT\mathbf{F}_\pm = \mathbf{F}_\mp$), then the eigenvalue ω is real. This, for example, can be achieved in systems with material parameters that change only along the z direction ($x \to x$, $y \to y$, $z \to -z$); for waves propagating along the z direction, we find that the conditions, so as to have a PT-symmetric chiral system, read as follows:

$$\varepsilon(z) = \varepsilon^*(-z), \quad \mu(z) = \mu^*(-z), \quad \kappa(z) = -\kappa^*(-z). \tag{1}$$

The reason for the minus sign in the last relation is the fact that κ is a pseudoscalar since it connects polar vectors ($\mathbf{E}$ and $\mathbf{D}$) to axial vectors ($\mathbf{B}$ and $\mathbf{H}$, respectively). The conditions Eq. (1) are a generalization of the conditions originally reported in Ref. [22] for nonchiral metamaterials and can be realized in practice, e.g., by homogeneously embedding chiral media in loss and gain, as depicted in Fig. 1. The system of Fig. 1 consists of two homogeneous chiral gain or loss slabs which are assumed to be infinite on the xy plane and have finite length along the z direction. Without loss of generality, gain (loss) is assumed to be embedded entirely in the left (right) slab.

To study the scattering properties of the double-slab system, we assume that circularly polarized waves arrive at normal incidence from either side of the system (propagating along the z direction) and measure the scattered fields. The amplitudes of the incident (b, c) and scattered (a, d) waves are shown in Fig. 1, where the subscript + (−) accounts for RCP (LCP) waves (the handedness is defined as seen from the source [34]). Although PT symmetry requirements impose certain relations [see Eq. (1)] between the coefficients in the loss and gain regions, we start with slabs of arbitrary lengths, L_g, L_l, and arbitrary material parameters ε_g, ε_l, μ_g, μ_l, κ_g, κ_l to obtain general expressions. Because of the two possible circular polarizations at each of the two sides, the system can be described by four input and four output ports and hence by a 4×4 scattering matrix, consisting of eight reflection and eight transmission amplitudes $\{r, t\}$. Regardless of the side of incidence, we find that $r_{++} = r_{--} = t_{+-} = t_{-+} = 0$, where the second subscript indicates the incident and the first the output polarization. For the remaining eight, nonzero scattering coefficients, we find

$$\begin{aligned}
&r_{L,+-} = r_{L,-+} \equiv r_L = r_{L,\text{nonchiral}},\\
&r_{R,+-} = r_{R,-+} \equiv r_R = r_{R,\text{nonchiral}},\\
&t_{L,++} = t_{R,++} \equiv t_{++} = t_{\text{nonchiral}} e^{+ik_0(L_g\kappa_g + L_l\kappa_l)},\\
&t_{L,--} = t_{R,--} \equiv t_{--} = t_{\text{nonchiral}} e^{-ik_0(L_g\kappa_g + L_l\kappa_l)},
\end{aligned} \tag{2}$$

where the subscript L or R denotes incidence from "left" or "right," respectively, and k_0 is the free-space wave number (the subscript nonchiral denotes the same system with $\kappa_g = \kappa_l = 0$). From Eq. (2) it is evident that, although the transmission is the same from both sides, as is typical in reciprocal systems [10], the reflection depends on the side of incidence. Note also that, while the reflection amplitudes are always identical to those of the nonchiral counterpart, the transmission amplitudes t_{++}, t_{--} are in general different, but can be made equal to $t_{\text{nonchiral}}$ if $L_g\kappa_g + L_l\kappa_l = 0$. In this case the system responds macroscopically as nonchiral, despite having local chirality; i.e., the local chirality is spatially balanced. We emphasize that the results Eq. (2) hold for slabs of general (not necessarily PT) geometrical and material parameters. The results for the scattering matrix simplify considerably and, as a result, its four

eigenvalues appear in two degenerate pairs (see Supplemental Material [39]):

$$\lambda_{1,2} = (r_L + r_R \pm \sqrt{(r_L - r_R)^2 + 4t_{++}t_{--}})/2. \quad (3)$$

From Eq. (2) we notice that $t_{++}t_{--} = t^2_{\text{nonchiral}}$, and hence, the scattering matrix eigenvalues are identical to those of the nonchiral counterpart for slabs of general (non-PT) geometrical and material parameters.

In general, due to the presence of gain and loss, $|\lambda_{1,2}| \neq 1$. However, if we apply PT conditions an exceptional point emerges, below which $|\lambda_1| = |\lambda_2| = 1$ (PT phase), while λ_1, λ_2 become an inverse conjugate pair above it, satisfying $|\lambda_1||\lambda_2| = 1$ [16,18] (broken PT phase). Because the eigenvalues are found to be independent of chirality, the exceptional point does not depend on chirality as well and, therefore, the PT aspect can be tuned independently from the chiral aspect. The experimental criterion introduced in Ref. [18] for locating the exceptional point is now expressed as

$$\frac{R_L + R_R}{2} - \sqrt{T_{++}T_{--}} = 1, \quad (4)$$

where $R_i \equiv |r_i|^2$, $i = \{R, L\}$, and $T_j \equiv |t_j|^2$, $j = \{++, --\}$. In addition, the generalized unitarity relation [18], which holds both below and above the exceptional point, is now expressed as

$$|\sqrt{T_{++}T_{--}} - 1| = \sqrt{R_L R_R}. \quad (5)$$

According to this expression there exists a flux-conserving scattering process for incident waves on a single side if and only if $\sqrt{T_{++}T_{--}} = 1$, and one of R_L or R_R vanishes, which is known as anisotropic transmission resonance (ATR) [18]. Although this holds for the mean quantity $\sqrt{T_{++}T_{--}}$, this process is not strictly flux conserving for excitation with only RCP or LCP waves, as $T_{++} \neq T_{--}$ when the PT conditions Eq. (1) are satisfied. However, inspection of Eq. (2) reveals that if $\text{Im}(L_g\kappa_g + L_l\kappa_l) = 0$, then $T_{++} = T_{--} \equiv T$, and flux-conserving ATRs are possible. This can be fulfilled if κ is not PT symmetric, while ε and μ are; it is a case beyond full PT symmetry.

As for the chiral features of our system, after applying Eq. (2) on the optical rotation $\theta = [\arg(t_{++}) - \arg(t_{--})]/2$ and ellipticity $\eta = (1/2)\sin^{-1}[(|t_{++}|^2 - |t_{--}|^2)/(|t_{++}|^2 + |t_{--}|^2)]$ [34], we find that θ depends only on the real part of κ, $\text{Re}(\kappa)$, and η only on its imaginary part, $\text{Im}(\kappa)$ (see Supplemental Material [39]). For PT-symmetric systems and for systems with properly balanced $\text{Re}(\kappa)$ [such as $\text{Re}(L_g\kappa_g + L_l\kappa_l) = 0$], θ is always zero, while the ellipticity of the transmitted wave can be tuned by adjusting $\text{Im}(\kappa)$ in the loss and gain slabs. When going beyond the full PT symmetry (i.e., only ε and μ being PT symmetric) in order to satisfy $\text{Im}(L_g\kappa_g + L_l\kappa_l) = 0$, η is always zero; i.e., the output wave is linearly polarized, while the optical activity can be tuned via $\text{Re}(\kappa)$ (or the length L of the slabs).

To demonstrate the above conclusions, let us consider a system that fulfills conditions Eq. (1), such as the system shown in Fig. 1, with $n_g = 2 - 0.2i$, $n_l = 2 + 0.2i$ (where $n = \sqrt{\varepsilon\mu}$) and $\kappa_g = -0.165 + 0.165i$, $\kappa_l = 0.165 + 0.165i$. The two slabs are of equal length $L_g = L_l = L/2$, and the eigenvalues of the scattering matrix, as well as the transmitted and reflected power, are shown in Fig. 2(a) as a function of the normalized frequency $\omega L/c$. The exceptional point, which separates the PT phase from the broken PT phase (shaded region), is located at $\omega L/c = 15.4$. Because of the symmetries imposed by Eq. (1) on the chirality parameter κ, $\text{Re}(\kappa)$ changes sign across the system. Hence, the optical rotation θ occurring in the first slab is subsequently canceled when the wave passes through the second slab, resulting overall in zero optical activity, $\theta = 0$, regardless of the location of the exceptional point. On the other hand, $\text{Im}(\kappa)$ preserves its sign across the entire system and, consequently, $\text{Im}(L_g\kappa_g + L_l\kappa_l) \neq 0$, resulting in $\eta \neq 0$ and, hence, $T_{++} \neq T_{--}$, as shown in Fig. 2(a). Practically, after the ATR located around $\omega L/c = 9.52$ (marked with a vertical dashed line), all higher ATRs are accompanied by $\theta = 0$ and $\eta = 45$ deg; i.e., there exist multiple operation points of zero reflection and full conversion of linearly polarized waves into circularly polarized

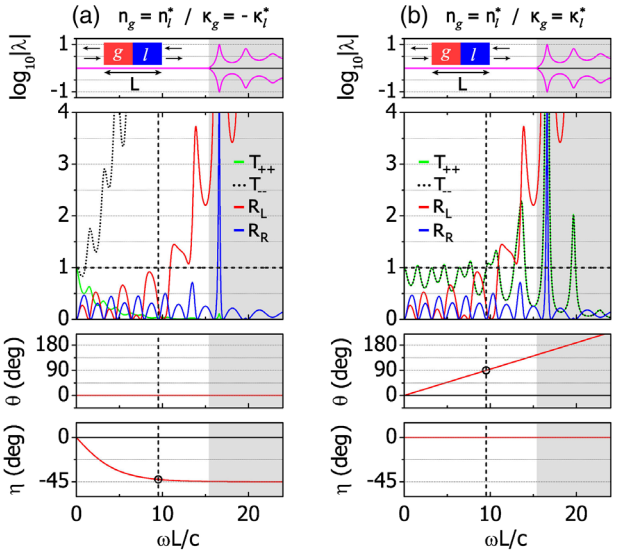

FIG. 2. PT-chiral system of length L with $n = 2 \pm 0.2i$. The chirality is (a) $\kappa = \pm 0.165 + 0.165i$ and (b) $\kappa = 0.165 \pm 0.165i$. Top row: Eigenvalues λ of scattering matrix. Middle row: Transmittance T_{++}, T_{--} and reflectance R_L, R_R. Bottom rows: Optical activity θ and ellipticity η. The generalized unitarity relation Eq. (5) is plotted as $R_L R_R + 2\sqrt{T_{++}T_{--}} - T_{++}T_{--} = 1$ (dashed horizontal line). The shaded area denotes the broken PT phase and the dashed vertical line marks an ATR with strong chiral features.

waves, the handedness of which is controlled by the sign of $\mathrm{Im}(\kappa)$.

Next, we relax the PT condition [last of Eq. (1)] by setting $\kappa_g = 0.165 + 0.165i$, $\kappa_l = 0.165 - 0.165i$. The sign change in $\mathrm{Im}(\kappa)$ leads to $\eta = 0$ (and $\theta \neq 0$) and $T_{++} = T_{--}$ without affecting the exceptional point, as predicted. We show below by simulation and retrieval in realistic chiral metamaterials that such choices are actually obtainable, and flux-conserving ATRs, as shown in Fig. 2(b), are possible, corresponding to unidirectional pure optical rotation of a linearly polarized wave. At the ATR around $\omega L/c = 9.52$, in particular (marked with a vertical dashed line), $\theta = 90$ deg; i.e., x-polarized waves are fully converted to y-polarized waves and are transmitted entirely without reflection.

To demonstrate our findings with realistic metamaterials, we employ a chiral metamaterial structure similar to the one presented in Ref. [35], which consists of two metallic crosses twisted with respect to each other by 30 deg and embedded in a dielectric host of low index, $n_{\mathrm{host}} = 1.41$ [see Fig. 3(a), top, for schematic and Supplemental Material for details [39]]. To achieve its PT counterpart (referred to here as PT CMM), we embed the dielectric host with gain (expressed as the imaginary part of n_{host}) and we also tune the relative twist between the two crosses for an additional control on the effective chirality, κ_{eff}. For $\mathrm{Im}(n_{\mathrm{host}}) = -0.09$ and an opposite twist of 30 deg between the two crosses [see Fig. 3(a), bottom], we achieve PT symmetry at 220 THz, as observed in the effective parameters $\varepsilon_{\mathrm{eff}}$, μ_{eff}, and κ_{eff} of the loss and gain CMMs in Fig. 3(b).

In particular, at this frequency we find $\varepsilon_{\mathrm{CMM}} = 0.365 + 0.299i$, $\varepsilon_{\mathrm{PT\text{-}CMM}} = 0.384 - 0.295i$, $\mu_{\mathrm{CMM}} = 1.527 - 0.149i$, $\mu_{\mathrm{PT\text{-}CMM}} = 1.549 + 0.037i$, and $\kappa_{\mathrm{CMM}} = 0.028 - 0.014i$, $\kappa_{\mathrm{PT\text{-}CMM}} = -0.030 - 0.007i$. To retrieve these parameters we use the procedure outlined in Ref. [35], for which we perform full-wave simulations with the commercial software COMSOL MULTIPHYSICS.

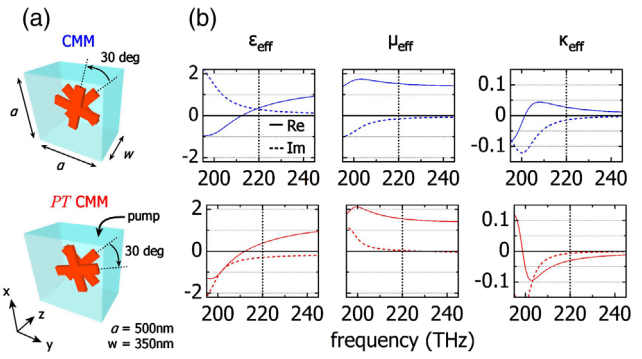

FIG. 3. (a) Unit cell of the basic CMM block (top) and its PT counterpart (bottom) satisfying the conditions Eq. (1) at 220 THz. The unit cell is periodically repeated on the xy plane. The length of the CMM along z direction is w. (b) Retrieved effective permittivity $\varepsilon_{\mathrm{eff}}$, permeability μ_{eff}, and chirality κ_{eff} as a function of frequency for the structures shown in (a). The results of the top (bottom) row correspond to the CMM (PT-CMM) system.

Next, we keep the PT-symmetric CMM pair intact and we introduce an additional nonmagnetic, nonchiral PT-slab pair ($\mu = 1$, $\kappa = 0$) of relative permittivity $\varepsilon' \pm i\varepsilon''$, to control the PT potential. The homogeneous slabs have $\varepsilon' = 2.1$ and are of 500 nm length each, so that the entire PT structure extends over a total of 1.7 μm (each CMM is 350 nm long). With this configuration, the PT transition can be implemented at a single frequency (220 THz) with varying the values of gain and loss, i.e., ε'' (note that the optical potential involves both the frequency and the material parameters). The results are shown in Fig. 4(a), where the schematic on top denotes the four different material regions.

As we tune ε'', we observe an exceptional point at $\varepsilon'' = 0.88$ and an ATR close to $\varepsilon'' = 1$ (with $R_R = 0$). The optical rotation θ is everywhere close to zero as is imposed by the PT conditions, and the available chirality at this frequency leads to a relatively weak ellipticity of $\eta = 2.5$ deg (this is not a limitation, as η can be very large in such systems—see Supplemental Material [39]). The dashed line in the bottom left-hand panel of Fig. 4(a) is the calculated generalized unitarity relation Eq. (5). The slight quantitative deviations observed in θ, η, λ, and Eq. (5)

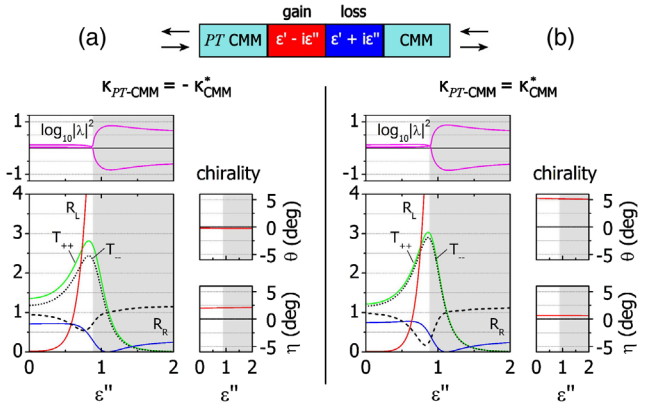

FIG. 4. Demonstration of PT transition (exceptional point) with a realistic PT-chiral metamaterial pair in terms of ε'', the imaginary part of the permittivity of the auxiliary gain or loss slab pair (the real part $\varepsilon' = 2.1$ is constant). The shaded area denotes the broken PT phase. (a) Numerical calculations at 220 THz for the CMM and PT-CMM blocks of Fig. 3 in the configuration shown in the schematic on top. (b) Results with the same CMM and the modified PT CMM, which has chirality of inverted sign. Panels: Scattering matrix eigenvalues λ (top left), transmittance T_{++}, T_{--} and reflectance R_L, R_R (bottom left), optical activity θ (top right), and ellipticity η (bottom right). The dashed line in the bottom left-hand panel is the quantity $R_L R_R + 2\sqrt{T_{++}T_{--}} - T_{++}T_{--}$. The relaxed PT condition in (b) does not affect the exceptional point, allowing for the PT aspect to be tuned independently from the chiral properties.

from the theoretically expected values (see Supplemental Material [39]), come from deviations of the retrieved parameters from the perfect PT conditions. However, the positions of the exceptional point and the ATR are not affected.

Because of $T_{++} \neq T_{--}$, the ATR observed in the system of Fig. 4(a) is not flux conserving for excitation with only RCP or LCP waves, as mentioned earlier. To achieve the condition $T_{++} = T_{--}$, which corresponds to $\eta = 0$ and thus pure optical rotation θ for a linearly polarized wave, we need to reverse the sign of chirality in the PT-CMM block, so that $\kappa_{\text{PT-CMM}} = (\kappa_{\text{CMM}})^*$; this obviously is an extension beyond the PT-invariance relation [last relation in Eq. (1)]. To demonstrate this possibility, we reverse the twist between the two crosses in the PT CMM, making it geometrically identical to the basic CMM (see Supplemental Material [39]). This modification changes the sign of $\kappa_{\text{PT-CMM}}$, without practically affecting $\varepsilon_{\text{PT-CMM}}$ and $\mu_{\text{PT-CMM}}$. The new parameters at 220 THz are $\varepsilon_{\text{PT-CMM}} = 0.356 - 0.293i$, $\mu_{\text{PT-CMM}} = 1.538 - 0.010i$, and $\kappa_{\text{PT-CMM}} = 0.031 + 0.0071i$. The simulations with the new system are shown in Fig. 4(b) and verify that the exceptional point is not affected by changes in chirality, as predicted by our simple model. Consequently, the properties of PT-symmetric systems are still possible, if PT-symmetry is obeyed by permittivity or permeability independently of PT being satisfied or not satisfied by the chirality κ. This conclusion is also verified in the existence of the flux-conserving ATR located close to $\varepsilon'' = 1$ (with $R_R = 0$).

In conclusion, we have shown that, despite the apparent incompatibility, the combination of chirality with PT symmetry in ε and μ is possible in certain systems, allowing thus the simultaneous exploitation of both. This exploitation is unrestricted as far as κ is concerned, since the chirality does not affect the eigenvalues of the scattering matrix and therefore leaves the functionalities related with the PT phase untouched. This unexpected κ independence of the PT phase has been shown to be of utmost importance, as it enables the simultaneous and independent control of both the PT-symmetric phase and chirality. Hence, the novel wave propagation and scattering properties of nonchiral PT-symmetric systems can be combined with the advanced polarization control properties of chiral metamaterials at will, allowing for the realization of several exciting possibilities, such as chiral unidirectional lasers and wave isolators of arbitrary polarization, in a very small scale.

This work was supported by the Hellenic Foundation for Research and Innovation (HFRI) and the General Secretariat for Research and Technology (GSRT), under the HFRI Ph.D. Fellowship grant (GA. No. 4820). It was also supported by the European Research Council under the ERC Advanced Grant No. 320081 (PHOTOMETA) and by the EU-Horizon2020 FET projects Ultrachiral and Visorsurf. Useful discussions with K. Makris are also acknowledged.

*sdroulias@iesl.forth.gr
†kafesaki@iesl.forth.gr

[1] C. M. Bender and S. Boettcher, Phys. Rev. Lett. **80**, 5243 (1998).
[2] C. M. Bender, S. Boettcher, and P. N. Meisinger, J. Math. Phys. (N.Y.) **40**, 2201 (1999).
[3] C. M. Bender, D. C. Brody, and H. F. Jones, Phys. Rev. Lett. **89**, 270401 (2002).
[4] C. M. Bender, Rep. Prog. Phys. **70**, 947 (2007).
[5] R. El-Ganainy, K. G. Makris, D. N. Christodoulides, and Z. H. Musslimani, Opt. Lett. **32**, 2632 (2007).
[6] K. G. Makris, R. El-Ganainy, D. N. Christodoulides, and Z. H. Musslimani, Phys. Rev. Lett. **100**, 103904 (2008).
[7] S. Klaiman, U. Günther, and N. Moiseyev, Phys. Rev. Lett. **101**, 080402 (2008).
[8] A. Guo, G. J. Salamo, D. Duchesne, R. Morandotti, M. Volatier-Ravat, V. Aimez, G. A. Siviloglou, and D. N. Christodoulides, Phys. Rev. Lett. **103**, 093902 (2009).
[9] E. Rüter, K. G. Makris, R. El-Ganainy, D. N. Christodoulides, M. Sagev, and D. Kip, Nat. Phys. **6**, 192 (2010).
[10] Z. Lin, H. Ramezani, T. Eichelkraut, T. Kottos, H. Cao, and D. N. Christodoulides, Phys. Rev. Lett. **106**, 213901 (2011).
[11] L. Feng, Y. L. Xu, W. S. Fegadolli, M. H. Lu, J. E. Oliveira, V. R. Almeida, Y. F. Chen, and A. Scherer, Nat. Mater. **12**, 108 (2013).
[12] Y. Shen, X. Hua Deng, and L. Chen, Opt. Express **22**, 19440 (2014).
[13] Y. D. Chong, Li Ge, Hui Cao, and A. D. Stone, Phys. Rev. Lett. **105**, 053901 (2010).
[14] Y. Sun, W. Tan, H. Q. Li, J. Li, and H. Chen, Phys. Rev. Lett. **112**, 143903 (2014).
[15] S. Longhi, Phys. Rev. A **82**, 031801(R) (2010).
[16] Y. D. Chong, L. Ge, and A. D. Stone, Phys. Rev. Lett. **106**, 093902 (2011).
[17] L. Ge, Y. D. Chong, S. Rotter, H. E. Türeci, and A. D. Stone, Phys. Rev. A **84**, 023820 (2011).
[18] Li Ge, Y. D. Chong, and A. D. Stone, Phys. Rev. A **85**, 023802 (2012).
[19] N. Lazarides and G. P. Tsironis, Phys. Rev. Lett. **110**, 053901 (2013).
[20] J. M. Lee, S. Factor, Z. Lin, I. Vitebskiy, F. M. Ellis, and T. Kottos, Phys. Rev. Lett. **112**, 253902 (2014).
[21] A. A. Zyablovsky, A. P. Vinogradov, A. A. Pukhov, A. V. Dorofeenko, and A. A. Lisyansky, Phys. Usp. **57**, 1063 (2014).
[22] G. Castaldi, S. Savoia, V. Galdi, A. Alu, and N. Engheta, Phys. Rev. Lett. **110**, 173901 (2013).
[23] S. Savoia, G. Castaldi, V. Galdi, A. Alu, and N. Engheta, Phys. Rev. B **89**, 085105 (2014).
[24] S. Savoia, G. Castaldi, V. Galdi, A. Alu, and N. Engheta, Phys. Rev. B **91**, 115114 (2015).
[25] J. Wang, H. Y. Dong, C. W. Ling, C. T. Chan, and K. H. Fung, Phys. Rev. B **91**, 235410 (2015).
[26] O. V. Shramkova and G. P. Tsironis, J. Opt. **18**, 105101 (2016).
[27] Y. Y. Fu, Y. D. Xu, and H. Y. Chen, Opt. Express **24**, 1648 (2016).
[28] C. M. Soukoulis and M. Wegener, Nat. Photonics **5**, 523 (2011).

[29] I. V. Lindell, A. H. Sihvola, S. A. Tretyakov, and A. J. Viitanen, *Electromagnetic Waves in Chiral and Bi-Isotropic Media* (Artech House Publishers Boston, MA, 1994).
[30] S. Tretyakov, I. Nefedov, A. Sihvola, S. Maslovski, and C. Simovski, J. Electromagn. Waves Appl. **17**, 695 (2003).
[31] J. B. Pendry, Science **306**, 1353 (2004).
[32] E. Plum, J. Zhou, J. Dong, V. A. Fedotov, T. Koschny, C. M. Soukoulis, and N. I. Zheludev, Phys. Rev. B **79**, 035407 (2009).
[33] J. Zhou, J. Dong, B. Wang, T. Koschny, M. Kafesaki, and C. M. Soukoulis, Phys. Rev. B **79**, 121104(R) (2009).
[34] B. Wang, J. Zhou, T. Koschny, M. Kafesaki, and C. M. Soukoulis, J. Opt. A **11**, 114003 (2009).
[35] R. Zhao, T. Koschny, and C. M. Soukoulis, Opt. Express **18**, 14553 (2010).
[36] G. Kenanakis, R. Zhao, N. Katsarakis, M. Kafesaki, C. M. Soukoulis, and E. N. Economou, Opt. Express **22**, 12149 (2014).
[37] E. Ozgun, A. E. Serebryannikov, E. Ozbay, and C. M. Soukoulis, Sci. Rep. **7**, 15504 (2017).
[38] E. U. Condon, Rev. Mod. Phys. **9**, 432 (1937).
[39] See Supplemental Material at http://link.aps.org/supplemental/10.1103/PhysRevLett.122.213201 for the analytical calculations and for additional numerical results.